

Modeling and Simulation of a Solar Tower Power Plant with Open Volumetric Air Receiver

Nils Ahlbrink Boris Belhomme Robert Pitz-Paal
German Aerospace Center, Institute of Technical Thermodynamics
Linder Hoehe, 51147 Cologne
nils.ahlbrink@dlr.de, boris.belhomme@dlr.de, robert.pitz-paal@dlr.de

Abstract

The start-up of the PS10 power plant in Seville, Spain, in 2007 marked the entrance of solar tower power plants into the commercial state. Questions about the right operational strategy, particularly during unsteady operation states, come to the fore, and therewith the need to carry out transient simulations of entire tower power plants including the heliostat field. Meeting this necessity, the presented simulation approach opens the way to transient full plant simulations of solar tower power plants. A detailed heliostat field model was linked to a dynamic receiver model by coupling both simulation tools. A second coupling was established to a tool hosting a control panel of the heliostat field model. With this simulation approach, a start-up procedure and a tracking stop were simulated delivering different transient behaviors of local absorber temperatures and mass flows.

Keywords: Solar tower, modeling, tool coupling, plant simulation

1 Introduction

A detailed analysis of a full system out of heliostat field and receiver requires models, which represent both parts in an adequate, strong simulation environment. A fast raytracing tool, namely STRAL (Solar Tower Raytracing Laboratory) [1], is used to represent the heliostat field including optical characteristics as well as transient heliostat tracking.

For the receiver, the object oriented modeling language Modelica in combination with the simulation environment Dymola is applied to develop a transient, discretized receiver model. Modelica is an object-oriented modeling language designed for modeling of complex physical systems [2], [3]. Dymola interprets the modeling language Modelica and enables for convenient dynamic simulations of complex systems [4]. An object-oriented model library

was developed for solar tower power plants with open volumetric air receiver technology, including the receiver, blowers, valves, pipes, the thermal storage system, and the power block. In combination with a heliostat field model, a complete solar tower power plant can be simulated [5]. The library is based on the open source Modelica library Modelica_Fluid [6].

The flux density distribution on the absorber surface of the receiver represents the physical interface between both models. To feed the receiver model with transient flux density data, both simulation environments need to be coupled. Therefore, STRAL was enhanced by an additional TCP/IP interface. An additional Dymola library was developed in parallel, enabling Dymola to communicate with STRAL via the same interface. In a second step, an additional tool coupling was established between STRAL and LabView for the purpose of a superior heliostat field control and human machine interface emulation.

The complete simulation system was tested running on three different computers. A solar tower power plant consisting of 153 heliostats and an open volumetric air receiver served as test case. The simulation scenario included a start-up procedure followed by a total heliostat field failure. During the failure time, the heliostats stopped tracking for 12 minutes and continued tracking afterwards.

The research results presented in this paper are part of a project, in which mainly control and operational strategies are developed for solar thermal power plants with open volumetric air receiver technology [5]. More information about the control strategy approach can be found in a related paper [7].

2 Transient system model

2.1 Heliostat field model

Like a couple of other well known flux density calculation tools for heliostat fields [8], the heliostat

field model used in STRAL [1] comprises effects as shading and blocking of heliostats as well. Furthermore each single heliostat model comprises an individual highly resolved heliostat geometry data set, obtained from deflectometry measurements, and in addition an individual transient tracking model of the heliostat drive system, meeting the fact of limited movement speeds and specific drive constellations. This enables to simulate transient effects as for instance during start-up procedures, aim point changes or even worst-case scenarios as partial or total failure of the heliostat field.

The used simulation consisted of 153 heliostats, each with a separate model of the heliostat drive system embedded in an external Dynamic Link Library. The heliostat field is shown exemplary in Figure 1. The actual azimuth rotation angle and elevation angle represent the two state variables of the simple drive system model. As can be seen in Equation 1, the actual axis rotation angle φ_{act} is incremented and decremented respectively with a constant axis rotation speed ω_{axis} until the target axis rotation angle φ_{tar} is reached. The target axis rotation angle φ_{tar} depends on the position of the heliostat relative to the receiver, the current sun position and on the actual aim point assignment.

$$\varphi_{act,t} = \begin{cases} \varphi_{act,t-1} + \omega_{axis} \cdot \Delta t, & \text{if } \varphi_{act,t-1} < \varphi_{tar} \\ \varphi_{act,t-1} - \omega_{axis} \cdot \Delta t, & \text{if } \varphi_{act,t-1} > \varphi_{tar} \\ \varphi_{tar}, & \text{if } \varphi_{act,t-1} = \varphi_{tar} \end{cases} \quad (1)$$

It is assumed that each axis of the heliostat is moved with a constant axis rotation speed ω_{axis} and effects as for instance overshooting are not considered. The simple approach is justified in this case since heliostats usually operate with very low axis rotation speeds.

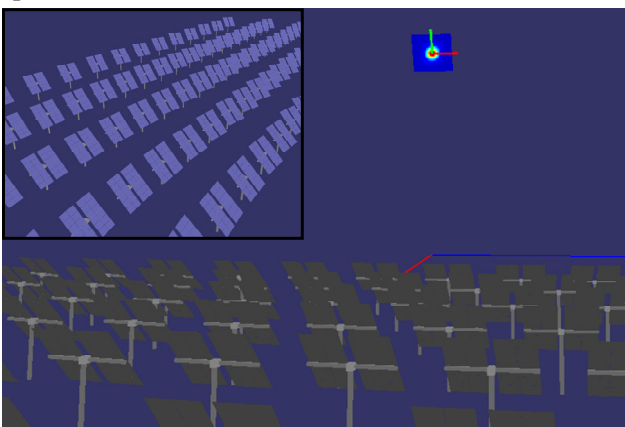


Figure 1 Heliostat field model in STRAL [1] showing the view towards the evaluation layer and upon the heliostat field (reduced window)

2.2 Receiver model

Depending on the purpose, the receiver can be modeled in different levels of detail. In this application, the dynamic behavior of the full receiver is the field of interest. Thus, the individual absorber components building the receiver are modeled in a more simplified way. Their individual temperature profile or the absorption process are not part of the investigations. The focus of the modeling is on the dynamic effects of the full receiver system including start-up, shut down and dynamic effects of an inhomogeneous flux density distribution in time and space. The main purpose of the model is to be used for analysis of transients in the receiver, for the development of control strategies, and for the prediction of receiver behavior.

Exemplary, a receiver with open volumetric air receiver technology is modeled. This technology uses a grid of absorber modules to setup a receiver. Analogously, the receiver model will use a representative number of absorber modules to model the full receiver as shown in Figure 2. A number of real absorber modules can be represented by one absorber module in the model. A matrix of $n \times m$ modules is set up to represent the receiver. The highest possible discretization is the real number of absorber module. Higher discretizations are disadvantageous, as the focus of the receiver model lies on the dynamic effects of the complete receiver system and not on the absorption and heat transfer processes inside the module. It would cost additional computation time. Using absorber modules as the smallest unit, receivers of different sizes can be simulated. Effects of up scaling can be analyzed.

The setup of the receiver model in Dymola is shown in Figure 3. In alternating sequence, flow and volume elements are instantiated according to [2].

Model of the absorber module

The key model of the receiver is the absorber module model (Figure 2). Two air streams are modeled; the first stream represents the air inside the module, which is heated up in the absorber comb, and the second stream represents the return air at the outside of the module, which is lead back to ambient cooling the receiver structure. The return are is fed back to the receiver from the cold air side of the power plant.

The absorption process and the heat transfer in the absorber comb have to be modeled very accurate, as the performance of the absorber module is mainly determined by the absorption efficiency besides mass flow rate and air inlet temperature. However, the complexity of the model should be as simple as

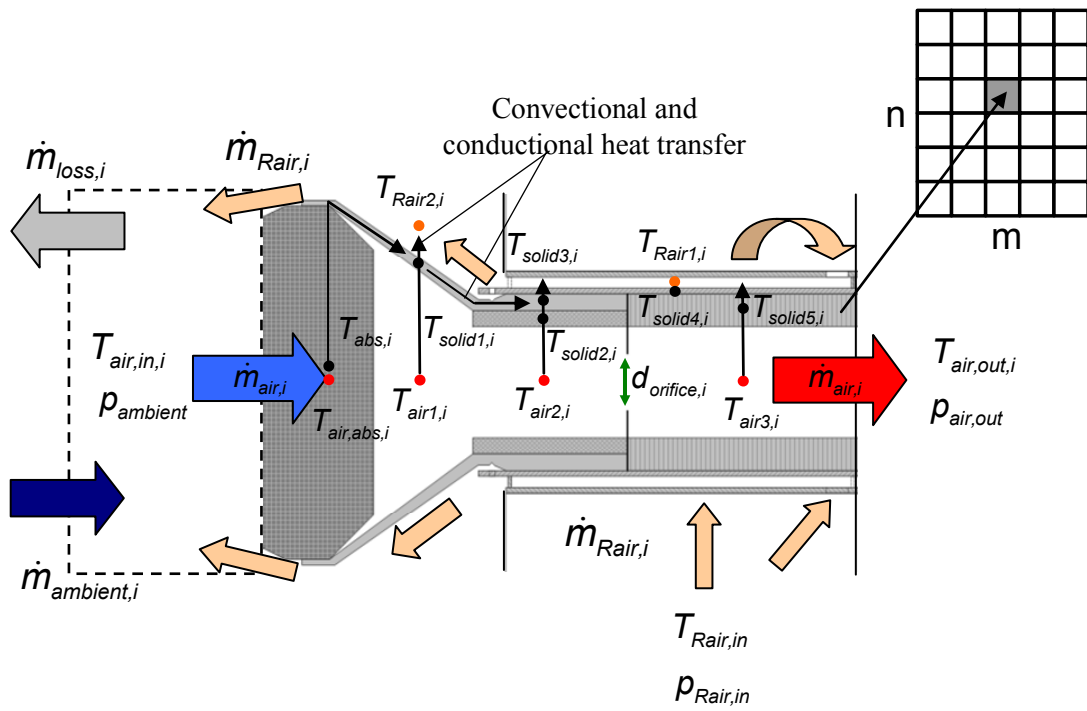


Figure 2: Absorber module model having 12 temperature nodes used for the receiver discretization of $n \times m$ absorber modules

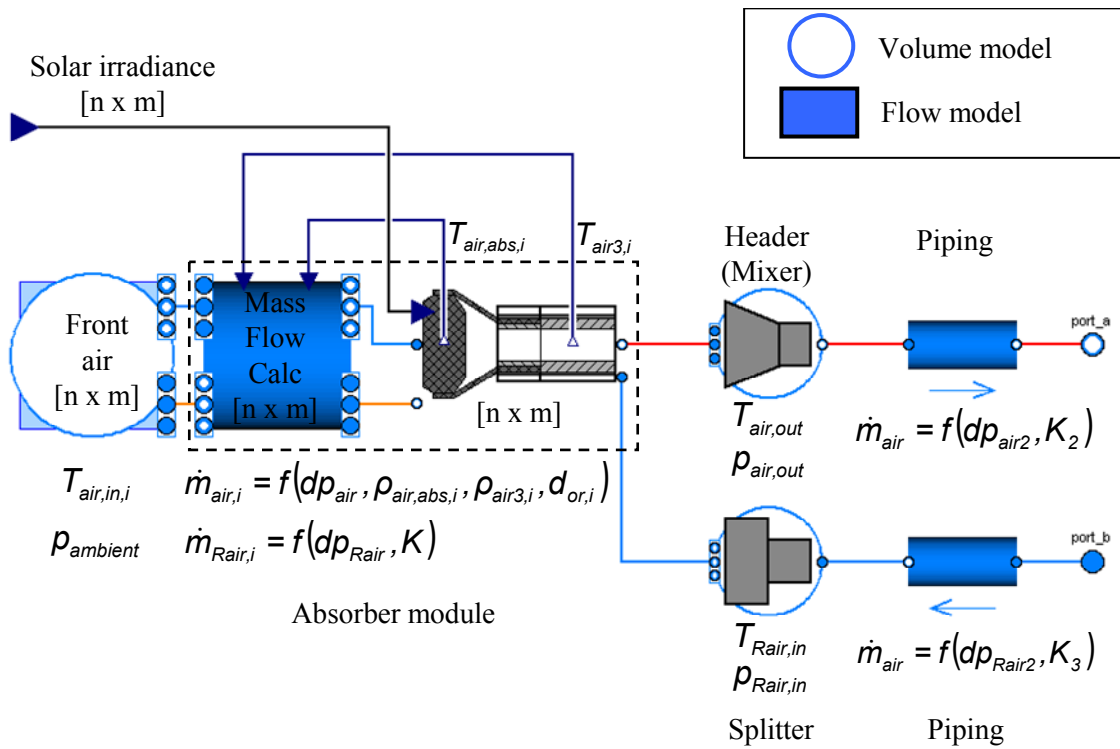


Figure 3: Schematic receiver model in Dymola including the described absorber module model

possible. Therefore, the absorption and heat transfer processes in the absorber comb are implemented by an efficiency interpolation matrix based on a detailed absorber model [9]. The inputs to the interpolation matrix are the flux density, the mass flow rate, and the inlet temperature. The result of the interpolation is the local efficiency from solar flux to heat absorbed in the absorber module.

Nusselt correlations are used for the heat transfer modeling between the hot air and the absorber cup, insulation, and the absorber pipe as well as for the heat transfer to the return air. 1-D heat conduction is assumed inside the solids in axial direction. In total, the absorber module model has 12 temperature nodes in the air streams and the solids. Depending on the up-coming model evaluation process, the number of nodes might be further reduced. Pressure at the nodes is assumed to be equal to the outlet pressure level $p_{air,out}$ for the main stream and the inlet pressure level $p_{Rair,in}$ for the return air. The pressure loss inside the modules is small, which results in a negligible influence on the fluid properties.

Mass flow rate distribution across receiver

Mass flow rate distribution across the receiver and the individual mass flow rates of the modules have a significant impact on the performance of the system. The mass flow rates of the individual absorber modules are dependent on each other since they are driven by a common pressure difference. The overall mass flow rate is split up into the absorber modules according to flow resistance of the modules. If the flow resistance of one module changes, for example by a changing flux density followed by an adapting air temperature, a new mass flow rate distribution over the receiver will establish. Thus, the absorber modules can not be considered individually.

In the absorber modules, like shown in Figure 2, a fixed orifice is used to adapt the mass flow rate according to a design flux density. Larger orifices are used in the center of the receiver as higher flux densities are expected. Smaller orifices are implemented in the less irradiated areas to achieve a desired temperature profile in the receiver at least for the design point flux density distribution. However, the orifices are not adaptable during operation, which results in deviant temperature profiles in off-design operating points.

The individual mass flow rates for the main air are modeled depending on the pressure difference Δp_{air} , the air densities in the absorber comb $\rho_{air,abs,i}$ and behind the orifice $\rho_{air3,i}$, and the orifice diameter $d_{orifice,i}$.

$$\begin{aligned} \dot{m}_{air,i} &= f(\Delta p_{air}, \rho_{air,abs,i}, \rho_{air3,i}, d_{orifice,i}) \\ &= \frac{-a + \sqrt{a^2 + 4b\Delta p_{air}}}{2b} \end{aligned} \quad (2)$$

The coefficients a and b are dependent on the densities, whereas factor b is as well a function of the orifice diameters $d_{orifice,i}$.

For the return air, a quadratic reference pressure drop model is used.

$$\begin{aligned} \dot{m}_{Rair,i} &= f(\Delta p_{Rair}, K) \\ &= \sqrt{\frac{\dot{m}_{Rair,Ref}^2}{\Delta p_{Rair,Ref}} \Delta p_{Rair}} \end{aligned} \quad (3)$$

For both air streams, it is assumed that the pressure difference is the same for all absorber modules.

$$\begin{aligned} \Delta p_{air} &= \Delta p_{air,i} = p_{ambient} - p_{air,out} \\ \Delta p_{Rair} &= \Delta p_{Rair,i} = p_{Rair,in} - p_{ambient} \end{aligned} \quad (4)$$

In Modelica, the receiver model is implemented according to flow and volume elements strategy [2]. Flow elements determine the mass flow rate while they do not store mass. Volume elements, however, account for storage effects but not for flow calculations. In our case, the flow elements calculate the mass flow rate out of the pressure difference according to two adjacent volume elements. In the volume elements, the pressure is used as a state variable. The second state variable in the volume elements is either the temperature or the specific enthalpy. Flow elements can have an energy balance as well.

Boundary condition at inlet of absorber module

In front of the receiver, the front air is modeled with a volume element according to the discretization with $n \times m$ volumes. It uses ambient pressure level. The air inlet temperature $T_{air,in,i}$ to the absorber modules is calculated. A part of the outflowing return air can be sucked in again. The amount is defined by an air return ratio. The other part is lost to ambient. Air from ambient mixes with the return air. The air inlet temperature to the absorber modules is a crucial variable for the performance of the absorber module. In the next step, a more detailed modeling of the effects of the air in front of the receiver will be implemented for example the rise of the hot air by natural convection.

The front air model is connected to the absorber module model, which uses the same discretization with $n \times m$ modules. It consists of two parts. As the absorber module model corresponds from its purpose to a flow model, the first block calculates the mass flow rates for both air streams and for each absorber

module. The second block represents the described absorber module setup having 12 temperature nodes.

The separation is used to be able to optimize the mass flow rate distribution calculation regarding calculation time in one central component in the future. The thermal behavior of the modules can be exchanged separately. At the moment, the calculation of the mass flow rate results in a very complex equation system as all flows are dependent on each other and on the air temperature or rather the flux density.

Pressure is, as described earlier, not a state variable in the absorber modules. The pressure change is neglectable for the fluid property calculation. That way the correct pressure difference is transferred to the mass flow rate calculation block according to equation 4. Two temperatures, the air temperature in the absorber comb $T_{air,abs,i}$ and the air temperature behind the orifice $T_{air3,i}$, are fed back to the temperature dependent mass flow rate calculation.

Boundary condition at outlet of absorber modules

The lumped air volume behind the absorber module in the main stream represents the header. Heat losses are modeled by Nusselt correlations. Pressure and specific enthalpy are the state variables for the volume for which balance equations are solved. The mass flow rates of the individual absorber modules are mixed in the header. It is followed by a pipe model. On the return air side, an equivalent setup is formed by a volume representing the air in the splitter and the return pipe.

2.3 Tool coupling of Dymola and STRAL

Both simulation tools, STRAL incorporating the detailed heliostat field model and Dymola incorporating the complete receiver and air cycle model, are to be used in one overall simulation. For that purpose, a tool coupling had to be established. It works via a TCP/IP network connection. To be able to control the heliostat field during the simulation run, for instance to modify the aim point configuration of the heliostats, a second connection is established between STRAL and LabView as shown in Figure 4.

The tool coupling is based on a classical client server model approach, where Dymola acts as Client, LabView as Server and STRAL as Server and Client at the same time. Therefore, a specific heliostat field model class was implemented in Dymola, incorporating an external static library, which is linked to the STRAL TCP/IP interface. The class makes use of the external function interface in Modelica [10].

A simulation run is divided into an initialization stage and a main simulation stage. During the initialization stage, the Dymola client establishes a connection to the STRAL server and passes initial conditions, as for instance specific receiver configurations (size, expected flux density discretization). Then, STRAL establishes a second connection to the LabView server, acting as client. The succeeding simulation stage is a sequence of calculations steps with modifiable time steps defined by the Dymola model. A model, which triggers events at specific time instants, evokes a calculation step. The step size of the events can be set for specific time periods.

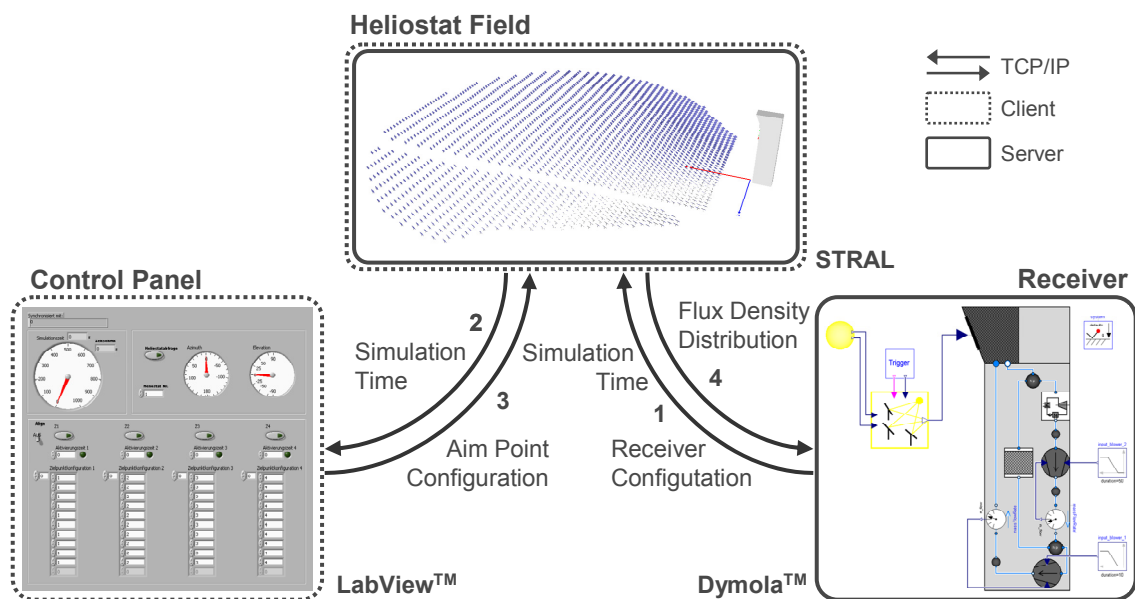


Figure 4: Tool Coupling Scheme of Dymola, STRAL and LabView

At the beginning of a single calculation step, Dymola sends a flux density calculation request to the STRAL server. This includes the actual simulation time and, optionally, the suns azimuth and elevation angle. If not defined by Dymola, the sun trajectory can be read directly in STRAL. In the following step, the STRAL client sends a synchronization request to the LabView server providing the actual simulation time as well. The LabView Heliostat Field Control Panel Application exchanges status data of the heliostat field and, if needed, modifies the configuration of the field, as for instance the current aim point assignment. After this procedure, the heliostat alignment is updated by STRAL considering the specified drive system model of each heliostat. Then the requested flux density calculation is calculated based on STRAL's raytracing engine. The resulting flux density distribution is send back to the Dymola application. Independently from the main calculation steps, Dymola performs variable integration time steps inside of the Dymola model.

In addition to the described standard procedure, STRAL can calculate the next flux density distribution in advance based on the step size of the last call. At the next calculation request, it will check the desired time step, sun position and aim point configuration, and compares it to the assumed next calculation steps. That way, the next step can be calculated in advance before Dymola actually requests the next calculation step. No waiting time occurs for the Dymola model to wait for the STRAL answer, in case the time step and aim point configuration has not been changed, which is normally the case.

3 Generic test case

The start-up of a power plant, consisting of the described receiver model in Dymola and a heliostat field model in STRAL, was simulated. A control panel, modeled in LabView was used to interact with the heliostat field model to be able to shift the aim points.

The Dymola model includes the receiver, an adjustable heat sink to cool down the air to a design air temperature after the receiver, and a blower. The heat sink is implemented instead of a consumer like a thermal storage or a steam generator. The design return air temperature is set to 110°C. The mass flow rate of the receiver is adjusted by the blower power. It is increased at the beginning within one minute to the overall design mass flow rate of 2.2 kg/s. It is kept constant by a controller during the simulation. Mass flow rate disturbances are caused by changes of the air temperature in the absorber modules due to

inhomogeneous irradiation. The mass flow rate distribution is dependent on the orifice diameters as well as the fluid properties and changes during the simulation.

The flux density is the input to the receiver, which is calculated by the heliostat field model. A discretization of 6x5 absorber modules is chosen. Each of the modules represents a matrix of 3x3 absorber modules. Thus, in total, 270 absorber modules of the real receiver are represented by 30 absorber modules in the model. For each of the modules, a specific orifice diameter was chosen depending on the location in the receiver. Larger diameters are used in the center to take care of expected higher flux densities and smaller diameters are implemented towards the edges of the receiver. The orifice diameters are important for the mass flow rate distribution, but cannot be adjusted during the simulation.

The Dymola model provides the receiver dimensions and discretization as well as the sun azimuth and elevation angle for the heliostat field model. The heliostat field model is set up in STRAL. It includes the 153 heliostats with a mirror area of 38.8 m² each. The heliostats have a constant rotation velocity of 0.01 mrad/s for the azimuth and elevation axis. At the beginning of the simulation, the heliostats point towards one common standby aim point west of the receiver surface. The aim point is shifted towards the center of the receiver, after the design mass flow rate is reached. The air temperatures inside the absorber modules will increase and approach a steady state level. At steady state level, a tracking stop of 12 minutes is simulated. The tracking stop represents possible mistakes or failure in the heliostat field control. In this scenario, the tracking is reactivated after 12 minutes, so that the heliostat focus is adjusted to the aim point at the center of the receiver again.

Figure 5 shows the solar irradiation, the material temperatures of five absorber modules in one receiver row and the average air outlet temperature, as well as the corresponding air mass flow rates. The locations of the absorber modules are displayed. They are positioned on the same horizontal axis in the fourth row of the receiver.

During the simulation, the material temperatures increase as the flux densities rise after shifting the aim point to the center. The shifting process is relatively fast compared to the temperature rise. Therefore, the solar irradiation increase appears similar to a step input. The temperatures increase and approach a steady state level. The start-up takes about 15 minutes for a temperature change of 800 °C. In this start-up procedure, all heliostats are shifted to one central aim point at the same time. As demonstrated, it causes a high temperature increase and therewith

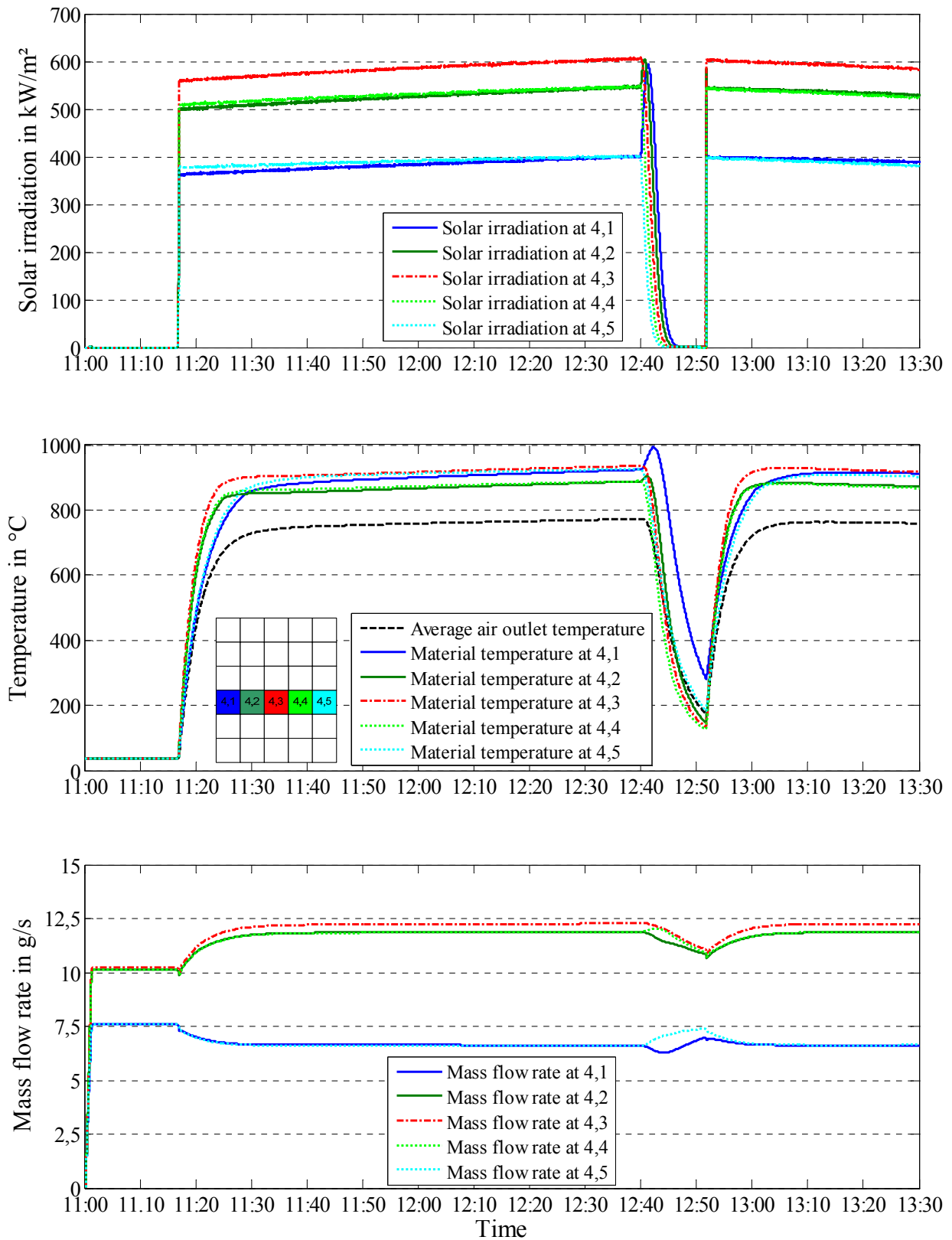


Figure 5: Solar irradiance, absorber material temperatures of five representative absorber modules of an open volumetric air receiver (6x5 total receiver discretization) and the average air outlet temperature, and the corresponding air mass flow rates of the five modules. The absorber modules have different orifice diameters and are located on the eastern side (4, 1) and (4, 2), in the center (4, 3) and on the western side (4, 4) and (4, 5) of the receiver in the fourth row. One module represents a matrix of 3 x 3 absorber modules.

high thermal stresses in the material. Other possible start-up procedures can be analyzed to define a more smooth and conservative start-up behavior.

From 12:40 ongoing, a tracking failure of 12 minutes is simulated. The heliostats remain in a fixed position. The focus of the irradiation moves towards the eastern edge of the receiver. The solar irradiation decreases immediately for the absorber module at the western edge and in the center of the receiver. In contrast, the irradiation on the module at the eastern edge increases with the focus moving towards the eastern edge. The temperatures follow the described behavior with a short time delay. An increase of around 70°C can be seen for the module at the eastern edge within some minutes. The temperature decreases as well, when the focus has shifted to the outside next to the receiver. After 12 minutes, the tracking is reactivated. The heliostats approach the aim point at the center of the receiver very fast. The temperatures increase to their previous level with time delay. The temperature rise is relatively small as the irradiation changes are manageable and a small receiver has been analyzed. In larger receiver, larger differences in mass flow rate and irradiation can occur. Unfortunately, the effects of irradiation changes are intensified.

The mass flow rate of each absorber module is dependent on the orifice diameter of the module and the air density. As the overall mass flow rate is kept constant, the individual mass flow rate of the modules changes with the temperature. The mass flow rates of the outer modules (4, 1) and (4, 5) decrease after the aim point shift, as they have a smaller orifice diameter as the central modules. The effect of rising temperatures is larger.

A similar phenomenon can be seen during the tracking failure. The modules on the eastern side with increasing irradiation show decreasing mass flow rates, the ones on the western side increasing mass flow rates until the focus of irradiation has left the receiver area. However, this time the orifice diameters are not well suited for this situation. Different temperature levels are reached. The material temperature of the module (4, 1) reaches a higher level leading to higher thermal losses. In order to be able to optimize the receiver behavior, adjustable orifices or air flaps could be implemented. That way, the mass flow rate distribution can be adjusted according to the irradiation conditions.

The simulation of a tracking stop was chosen to demonstrate one possible problem and its consequences during operation of a heliostat field. Problems like this can lead to temperature gradients in the receiver, which cannot be neglected. They can even cause great damage. In this specific case, the destruc-

tive temperature levels are not reached. It might still be necessary for other configurations to install an emergency defocusing of the heliostat field which still operates in case of an electrical power outage for the heliostat field and in case the blower fails as well.

4 Conclusions

For the first time, transient simulation of a solar tower power plant including heliostat field and a discretized solar receiver is described. A tool coupling was developed linking two simulation environments, namely STRAL representing the heliostat field and Dymola representing the receiver. Additionally, a second coupling was established to link a heliostat field control modeled in the LabView environment.

A detailed receiver model for the transient behavior of an open volumetric air receiver has been developed as one part of a Modelica model library. The structure of the absorber modules as the key components of the receiver is discussed as well as the implementation of the receiver in a Modelica model.

The simulation of a test case, comprising the start-up procedure and a tracking failure of the entire heliostat field, was accomplished. Occasionally large temperature gradients could be detected in some absorber modules of the receiver, which could lead to critical operation conditions. These exemplary results underline the necessity to carry out transient simulations of the entire solar tower power plant, especially during changing operational conditions, as for instance during start-up, failures or cloud passing.

References

- [1] Belhomme, B., Pitz-Paal, R., Schwarzbözl, P., Ulmer, S. (2009): A new fast Ray Tracing Tool for High-Precision Simulation of Heliostat Fields, *Journal of Solar Energy Engineering*, 131 (3), 2009, in Press
- [2] Tummescheid, H. (2002): Design and Implementation of Object-Oriented Model Libraries using Modelica. Thesis, Department of Automatic Control, Lund Institute of Technology, Lund, August 2002
- [3] Modelica Association (2009): Modelica® - A Unified Object-Oriented Language for Physical Systems Modeling, Language Specifications, Version 3.1, May 27th, 2009

- [4] Dynasim AB (2004): Dymola Version 7.1
<http://www.dynasim.se>
- [5] Ahlbrink, N., Alexopoulos, S., Andersson, J., Belhomme, B., Boura, C., Gall, J., Hirsch, T. (2009): vICERP – The virtual Institute of Central Receiver Power Plants: Modeling and Simulation of an Open Volumetric Air Receiver Power Plant. Conference Proceedings, MATMOD Conference 2009, 263, Vienna, February 11-13, 2009
- [6] Casella, F., Otter, M., Proelss, K., Richter, C., Tummescheid, H. (2006): The Modelica Fluid and Media library for modeling of incompressible and compressible thermo-fluid pipe networks. Conference Proceedings, Modelica Conference 2006, 631-640, Vienna, September 4-5 2006
- [7] Schmitz, M., Boura, C., Ahlbrink, N., Gall, J., Andersson, J. (2009): Optimized control of a hot –gas cycle for solar thermal power plants. Conference Proceedings, Modelica Conference 2009, Como, September 20-22, 2009, in Press
- [8] Garcia, P., Ferriere, A. (2008): Codes for Solar Flux Calculation dedicated to Central Receiver System Application: A comparative Review, Journal of Solar Energy, 3 (2008) 189-197
- [9] Hoffschmidt, B. (1997): Vergleichende Bewertung verschiedener Konzepte volumetrischer Strahlungsempfänger. Forschungsbericht / Deutsches Zentrum für Luft- und Raumfahrt e.V.; 1997, 35, Köln: DLR, 1997. 212 S.: ISBN: 1434-8454; Aachen, Technische Hochschule, Diss.; Reportnr.: DLR FB 97 35
- [10] Fritzson, P. (2004): Principles of object-oriented modeling and simulation with Modelica 2.1. Wiley-IEEE Press, 2004